LBL-1415
c.2

DETERMINATION OF LOOP TYPE IN As^+ IMPLANTED SILICON

Wei-Kuo Wu
(M.S. Thesis)

February 1973

Prepared for the U.S. Atomic Energy Commission
under Contract W-7405-ENG-48

TWO-WEEK LOAN COPY

This is a Library Circulating Copy which may be borrowed for two weeks. For a personal retention copy, call Tech. Info. Division, Ext. 5545

LBL-1415
c.2

DISCLAIMER

This document was prepared as an account of work sponsored by the United States Government. While this document is believed to contain correct information, neither the United States Government nor any agency thereof, nor the Regents of the University of California, nor any of their employees, makes any warranty, express or implied, or assumes any legal responsibility for the accuracy, completeness, or usefulness of any information, apparatus, product, or process disclosed, or represents that its use would not infringe privately owned rights. Reference herein to any specific commercial product, process, or service by its trade name, trademark, manufacturer, or otherwise, does not necessarily constitute or imply its endorsement, recommendation, or favoring by the United States Government or any agency thereof, or the Regents of the University of California. The views and opinions of authors expressed herein do not necessarily state or reflect those of the United States Government or any agency thereof or the Regents of the University of California.

DETERMINATION OF LOOP TYPE IN As^+ IMPLANTED SILICON

Contents

Abstract iv

I. Introduction 1

II. Description of the Method 4

A. General Consideration 4

B. Sense of Tilting 4

C. Conclusions 5

III. Experiments 6

A. $p^+(2 \times 10^{14}/cm^2)$ Implanted Si After 750° Annealing for 1/2 Hour 6

1. Top Bottom and Slip Plane Method 6

2. Quick Method 6

3. Determination of Loop Type of p^+ Implanted Si . . . 7

B. $As^+(1 \times 10^{14}/cm^2)$ Implanted Si After 1 Hour Annealing at 800°C 8

1. Normal Site 8

2. Flipped Over 8

IV. Summary and Conclusion 9

Acknowledgements 11

References 12

Figure Captions 13

Figures 15

DETERMINATION OF LOOP TYPE IN As^+ IMPLANTED SILICON

Wei-Kuo Wu

Inorganic Materials Research Division, Lawrence Berkeley Laboratory and Department of Materials Science and Engineering, College of Engineering; University of California, Berkeley, California

ABSTRACT

Simple rules have been deduced making use of the Kikuchi pattern to determine the loop types of double-arc prismatic loops[1] of any size. With this method, small double-arc prismatic loops in As^+ implanted Si have been shown to be of interstitial type.

I. INTRODUCTION

Double-arc prismatic loops have been found in deformed or quenched materials and also in radiation damaged materials. For diamond cubic materials, the loop planes are of {111} type.

The two beam electron diffraction contrast image of the loops has an out of contrast line along one of the ⟨110⟩ directions in the loop plane.

The Burgers vectors for this kind of loop are inclined to the loop plane, lying along the ⟨110⟩ direction that is perpendicular to the out of contrast line. The details of double-arc contrast from dislocation loops of fcc, bcc and dc crystals are described in Ref. 1.

It is convenient to describe loop planes and Burgers vectors with the aid of the Thompson tetrahedron (see Fig. 1). The four faces of the tetrahedron are the possible loop planes while all the edges are the possible out of contrast line as well as possible Burgers vectors. Because for each of the ⟨110⟩ directions, there is only one other ⟨110⟩ that is perpendicular to it. Hence, Burgers vector can be determined from the direction of the out of contrast line.

Several methods have been described for distinguishing between vacancy and interstitial loops.[2,3]

The general rules for determining loop types following the convention of P. B. Hirsch, et al.[4] can be stated as (see Fig. 2):

1. $(\bar{g} \cdot \bar{b}) < 0$ For outside contrast (keeping S always positive)

   $(\bar{g} \cdot \bar{b}) > 0$ For inside contrast (keeping S always positive)

2. $\hat{b} \cdot \hat{n} > 0$ For vacancy type

$\hat{b} \cdot \hat{n} < 0$ For interstitial type

In Fig. 2, it is clear that in order to distinguish between these two types, one can tilt the specimen through a large angle so that one type will increase in size, while the other will decrease (usually called high angle tilting and stereomicroscopy method). Alternatively, if the loops are large enough, or if other reference planes are identified by a fault, or a precipitate that lies on a known crystallographic plane and extends through the foil, then the top and bottom of the foil can be determined from dark-field pictures at $S > 0$ or $S < 0$ (Fig. 3). This also permits the loop plane to be determined and therefore the loop type.[5]

More quantitatively, the sense of the Burgers vector can be determined by the first rule shown above. Also from Fig. 2, we find that no matter what type the loops are, the plane normals $\hat{n}$ are defined so that they always make an abtuse angle with the beam direction. Hence, knowing the beam direction, i.e., at right angles to the foil plane, the loop plane is uniquely determined. Finally, by the second rule, the loop type is determined right away. Thus far the only problem that is left unsolved is how to uniquely determine the foil orientation, i.e., $\bar{g}$ vectors.

For a given diffraction pattern, there always exists an 180° ambiguity that makes it impossible to uniquely determine the foil orientation directly.

The Kikuchi pattern[6,7,8] is not symmetrical along the ⟨220⟩ band on the two sides of the [111] pole (Fig. 4). Many authors have used

the Kikuchi pattern along with high angle tilting and stereomicroscopy to determine loop type. This is a rather inaccurate method for small loops unless other easily identifiable reference defects are available.

In this paper, for {111} foils in silicon, it is pointed out that only the Kikuchi pattern is necessary. High angle tilting and stereomicroscopy is unnecessary. If we know the relative position of two poles along the asymmetric ⟨220⟩ band, then we know exactly how the tetrahedron is oriented in the foil. For dc or fcc crystals near [111], the nearest asymmetric pole from [111] is only about 5°. Hence this method permits determination of loop types of prismatic loops in (111) foils in a very quick way. (Usually only 6 pictures are enough to identify all three sets of double-arc loops.)

This method has been tested with some known loop types in ion implanted silicon. In one case, the foil was also flipped over to show that this has no effect on the result.

II. DESCRIPTION OF THE METHOD

For simplicity, we shall only consider orientations near [111].

A. General Consideration

From Fig. 5, we can see that there are four possible ways that we can arrange the Thompson tetrahedron in order to get the Kikuchi pattern as shown. However, with the transformation matrix

$$\begin{vmatrix} 0 & \bar{1} & 0 \\ \bar{1} & 0 & 0 \\ 0 & 0 & \bar{1} \end{vmatrix} ,$$

the two tetrahedra shown on Fig. 6 have exactly the same parallel planes, but with their plane normals reversed in sign relative to the beam direction. Hence the four orientations of Thompson tetrahedron in Fig. 5 can be reduced to the two shown in Fig. 7(a) and Fig. 7(b). This means the tetrahedron can be considered as being in the [111] or the $[\bar{1}\bar{1}\bar{1}]$ orientation.

B. Sense of Tilting

From Fig. 8, it is clear that the relationship between the Kikuchi pattern and the Thompson tetrahedron should be as shown.

The Thompson tetrahedron for Fig. 8(a) should be oriented with the corners pointed opposite to {112} poles and with [111] up, while for Fig. 8(b) it should be with corners pointing toward $\{\bar{1}\bar{1}2\}$ poles with $[\bar{1}\bar{1}\bar{1}]$ up.

Also from Fig. 8, we can see that in order to see the {112} pole after tilting from {111} pole, the sense of movement in the Kikuchi pattern should be in a consistent way in both cases, i.e., the sense of tilting should be in the same direction as the direction of movement of the Kikuchi pattern.

Hence from Fig. 8, we can conclude that for a [111] oriented tetrahedron, the corners should be pointing away from the {112} pole while for $[\bar{1}\bar{1}\bar{1}]$ type tetrahedron the corners should be pointing toward the {112} pole.

C. Conclusions

We conclude that Fig. 7 can be further reduced to either $[\bar{1}\bar{1}\bar{1}]$ or [111].

Hence we conclude that in determining the loop type of double-arced loops we can assume either that the tetrahedron is as in Fig. 9(a) with [111] up and index all $\bar{g}$ vectors accordingly or that it is as in Fig. 9(b) with $[\bar{1}\bar{1}\bar{1}]$ up. Because of the equivalency, here after we shall use only $(\bar{1}\bar{1}\bar{1})$ up orientation to interpret all the micrographs.

This equivalency also means that it does not matter from which side the plate is viewed i.e. (whether the beam detection is taken correctly or opposite).

III. EXPERIMENTS

For phosphorus implanted silicon, two different methods have been used to determine the loop type. Both these methods come to the same results showing the loops to be of interstitial type. For As^+ implanted silicon loop type has not previously been determined. In the present experiments, with this new quick method for indexing $\bar{g}$ vectors without high angle tilting, the small loops in As^+ ($1 \times 10^{14}/cm^2$) implanted Si after 1 hour annealing at 800°C are also of interstitial type. The details of these experiments and the results are discussed in this section.

A. $p^+(2 \times 10^{14}/cm^2)$ Implanted Si After 750°C Annealing for 1/2 Hour

1. Top Bottom and Slip Plane Method

For p^+ implanted Si, there were many bar-shaped[9,10] defects along ⟨110⟩ as have been found in B^+ implanted Si.[11,12]

When S > 0 the bottom of the foil should be in stronger contrast. Those bars marked T. B. in Figs. 11 and 12 are inclined to the foil normal and along ⟨110⟩ with the end in good contrast marked B. Hence, the tetrahedron is oriented as shown in Fig. 12(c).

2. Quick Method

The series of pictures in Fig. 13 were taken with diffraction conditions as shown in Fig. 13(a). Hence, from the Kikuchi pattern, the tetrahedron is oriented as shown in Fig. 13(a). It is the same orientation arrived at in Fig. 12(c).

3. Determination of Loop Type of p^+ Implanted Si

a. The direction of $\bar{g}$ vectors on Fig. 13 were assigned by assuming $(\bar{1}\bar{1}\bar{1})$ orientation. The Burgers vectors for the three main kinds of loops are

$$\bar{b}_A = \pm\frac{a}{2}[011] \qquad \bar{b}_B = \pm\frac{a}{2}[110] \qquad \vec{b}_C = \pm\frac{a}{2}[101]$$

As shown in Fig. 13(b), when $\bar{g} = \{20\bar{2}\}$, A-type is of outside contrast while B-type is of inside. Hence, $\bar{b}_A = \frac{a}{2}[011]$ and $\bar{b}_B = \frac{a}{2}[110]$. Also, when $g = [0\bar{2}2]$, C type is of inside contrast. So, $\vec{b}_C = \frac{a}{2}[101]$.

For all those three kinds of loops, the plane normals should be either $(\bar{1}\bar{1}\bar{1})$, $(\bar{1}\bar{1}1)$, $(1\bar{1}\bar{1})$ or $(\bar{1}1\bar{1})$, but for any of those loop planes.

$$\vec{b}_i \cdot \vec{n} < 0 \qquad i = A.B.C.$$

Hence, all loops are of interstitial type.

b. If we assume that the tetrahedron is oriented with (111) up, then the $\vec{g}$ vectors should be assigned as shown in Fig. 13(a).

In this case, $\vec{b}_A = \pm\frac{a}{2}[110]$, $\vec{b}_B = \pm\frac{a}{2}[011]$ and $\bar{b}_C = \pm\frac{a}{2}\{101\}$.

Again from Fig. 13 with inside and outside contrast experiment, we can uniquely determine the Burgers vectors of those three types as:

$$\vec{b}_A = \frac{a}{2}[\bar{1}\bar{1}0] \qquad \vec{b}_B = \frac{a}{2}[0\bar{1}\bar{1}] \text{ and } \vec{b}_C = \frac{a}{2}[\bar{1}0\bar{1}]$$

And for this case, the plane normals should be taken as (111), $(\bar{1}11)$, $(1\bar{1}1)$ or $(11\bar{1})$.

However, no matter what the plane normal really is, we have $\vec{b}_i \cdot \vec{n} < 0$, i = A.B.C. which again implies that all those loops are of interstitial type.

B. As^+ ($1 \times 10^{14}/cm^2$) Implanted Si After 1 Hour Annealing at 800°C

For As^+ implanted Si, the loops formed after annealing at high temperature are very small in size, also there is no apparent slip planes or defects along crystallographic directions inclined to the foil as in the p^+ implanted Si. Hence, the quick method is utilized to determine the loop types. In this experiment, the first part is a sample with implanted face toward gun and in the second part, we use the same sample but flipped over. In both cases, the same method is used, and we found the same result.

1. Normal Site

In this case, the $\bar{g}$ is assigned with $(\bar{1}\bar{1}\bar{1})$ up as shown in Fig. 14(a), and the Burgers vectors were determined by inside and outside contrast to be as:

$$\bar{b}_A = \frac{a}{2}[110] \ , \ \bar{b}_B = \frac{a}{2}[101] \ , \ \vec{b}_C = \frac{a}{2}[011]$$

As far as the loop type is concerned, we found that $\vec{n} \cdot \vec{b}_i < 0$ i = A.B.C. which implies that they are of interstitial type.

2. Flipped Over

We use the same concept assuming that the tetrahedron is with $(\bar{1}\bar{1}\bar{1})$ up, as shown in Fig. 15(a), and find that:

$$\bar{b}_A = \frac{a}{2}[110] \ , \ \bar{b}_B = \frac{a}{2}[101] \text{ and } \bar{b}_C = \frac{a}{2}[011]$$

As in Section III-B-1, so far as loop type is concerned, $\vec{n} \cdot \vec{b}_i < 0$, i = A.B.C. which also implies that they are of interstitial type.

IV. SUMMARY AND CONCLUSION

1. For As^+ implanted silicon, it has been shown that all the dislocation loops forming on annealing after implantation are of interstitial type and it has been analyzed with the aid of high angle tilting that most of them lie on the {111} plane parallel to the surface of the foil and have Burgers vectors inclined to the plane of the foil.

2. According to the previous discussion and experiments, we conclude that we can state some simple rules for determing loop type in {111} foils for dc and fcc structures for the case where loops are known to lie on {111}.

   The rules are:

   a. Determine the direction of {112} poles from the Kikuchi pattern.

   b. Index the $\vec{g}$ vectors with the corners of the Thompson tetrahedron toward the {112} poles assuming that the $[\bar{1}\bar{1}\bar{1}]$ direction is up.

   c. Take photographs of loops using ⟨220⟩ reflection with +g and -g to determine Burgers vectors ($(\vec{g} \cdot \vec{b})\, s < 0$, for outside contrast).

   d. Then if:

      $\vec{b} \cdot \vec{n} < 0$ loops are of interstitial type

      or if:

      $\vec{b} \cdot \vec{n} > 0$ loops are of vacancy type (see Fig. 10)

3. The advantages of this method over others are:

   a. Only small angle tilting is necessary to know the sense of the Kikuchi pattern.

   b. Only simple plus $\vec{g}$ and minus $\vec{g}$ photographs are required.

4. All the above discussion has been limited to foil orientations near [111]. However, it should be possible to expand this concept to other poles for which similar rules could be deduced.
5. The only limitation of the use of this method is that there has to be Kikuchi pattern from the sample to be dealt with. For specimens that do not give a Kikuchi pattern, the method of " 2nd Laur zone "[13] can be used to determine the sense of the Kikuchi pattern, then the same method can be used to determine loop types.

ACKNOWLEDGEMENTS

The author wants to express his gratitude to Professor Jack Washburn for his encouragement and inspiration throughout this work. Also he wants to thank Mr. Lih Juann Chen for his pertinent discussions. He is also grateful to Dr. Reddi and Fairchild Camera and Instrument Corporation for supplying the arsenic ion implanted silicon. Special thanks to Professor G. Thomas for his discussions and suggestions.

This work was done under the auspices of the U. S. Atomic Energy Commission through the Inorganic Materials Research Division of the Lawrence Berkeley Laboratory.

REFERENCES

1. G. Thomas and W. L. Bell, Lattice Defects and Their Interactions (Gordon and Breach, New York, 1967) p. 477.

2. G. W. Grove and A. Kelly, Phil. Mag. 6, 1527 (1961); Phil. Mag. 7, 892 (1962).

3. D. J. Mazey, R. S. Barnes and A. Howie, Phil. Mag. 7, 1861 (1962).

4. P. B. Hirsch, et al., Electron Microscopy of Thin Crystals (Butterworths, London, 1965) p. 266.

5. W. L. Bell and G. Thomas, Phys. Stat. Sol. 12, 843 (1965).

6. E. Levine, W. L. Bell and G. Thomas, J. Appl. Phys. 37, 2441 (1966).

7. G. Thomas, Kikuchi Electron Diffraction and Applications, in Modern Diffraction and Imaging Techniques in Materials Science (North-Holland, 1970) p. 159.

8. G. Thomas, Met. Trans. AIME 233, 1608 (1965).

9. K. Seshan and J. Washburn, Radiation Effects 14, 267 (1972).

10. M. Tamura, T. Klkeda and T. Tokuyama, 2nd International Conference on Ion Implantation in Semiconductors, p. 96.

11. R. W. Birknell and R. M. Allen, Rad. Effects 6, 45 (1970).

12. L. T. Chadderton and F. H. Eisen, Rad. Effects 7, 129 (1971).

13. M. vonHeimendahl, Phys. Stat. Sol. (a)5, 137 (1971).

FIGURE CAPTIONS

Fig. 1. Thompson tetrahedron.

Fig. 2. Relationship between loop type and contrast following the convention of P. B. Hirsch, et al.[4]

Fig. 3. Relationship of contrast at top or bottom of foil surface at $S < 0$ or $S > 0$ in dark field.

Fig. 4. Kikuchi pattern of (111). (Courtesy of J. Appl. Phys.[6])

Fig. 5, 7 and 9. Showing relationship between Kikuchi pattern and Thompson tetrahedron.

Fig. 6. Showing relationship between two Thompson tetrohedrons of parallel planes but different orientations.

Fig. 8. Showing relationship among Thompson tetrahedron, Kikuchi pattern and Stereographic projection.

Fig. 10. Table of contrast changes between vacancy and interstitial type at different $\bar{g}$ vectors.

Fig. 11 Dark field pictures showing that at $S > 0$ diffraction condition, the bottom (marked B) of the rod defects along ⟨110⟩ direction inclined to the foil.

Fig. 12(a) Dark field pictures showing that at $S > 0$ diffraction condition, the bottom (marked B) of the rod defects along ⟨110⟩ direction inclined to the foil.

Fig. 12(b) Those inclined rod defects along ⟨110⟩ crystallographic directions tell how the Thompson tetrahedron is oriented.

Fig. 13(a) SAD near (111) and the corresponding Kikuchi pattern and the orientation of Thompson tetrahedron relative to the given Kikuchi pattern.

Fig. 13(b),(c) and (d) Showing sequence of P^+ implanted Si with different $\vec{g}$ vectors as indicated.

Fig. 14(a) SAD near (111) and the corresponding Kikuchi pattern and the orientation of Thompson tetrahedron relative to the given Kikuchi pattern.

Fig. 14(b) and (c) Showing sequence of P^+ implanted Si with different $\vec{g}$ vectors as indicated.

Fig. 15(a) SAD near (111) and the corresponding Kikuchi pattern and the orientation of Thompson tetrahedron relative to the given Kikuchi pattern.

Fig. 15(b),(c) and (d) Showing sequence of As^+ implanted Si with different $\vec{g}$ vectors as indicated.

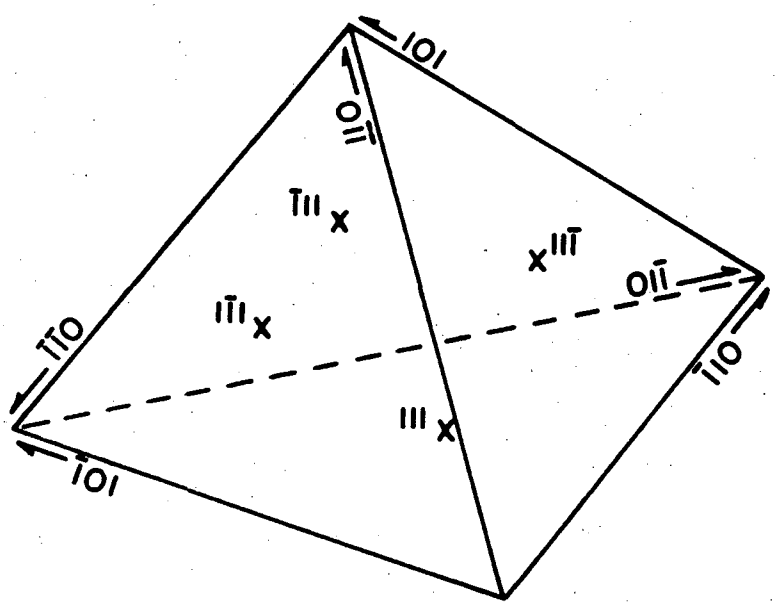

XBL731-5611

Fig. 1

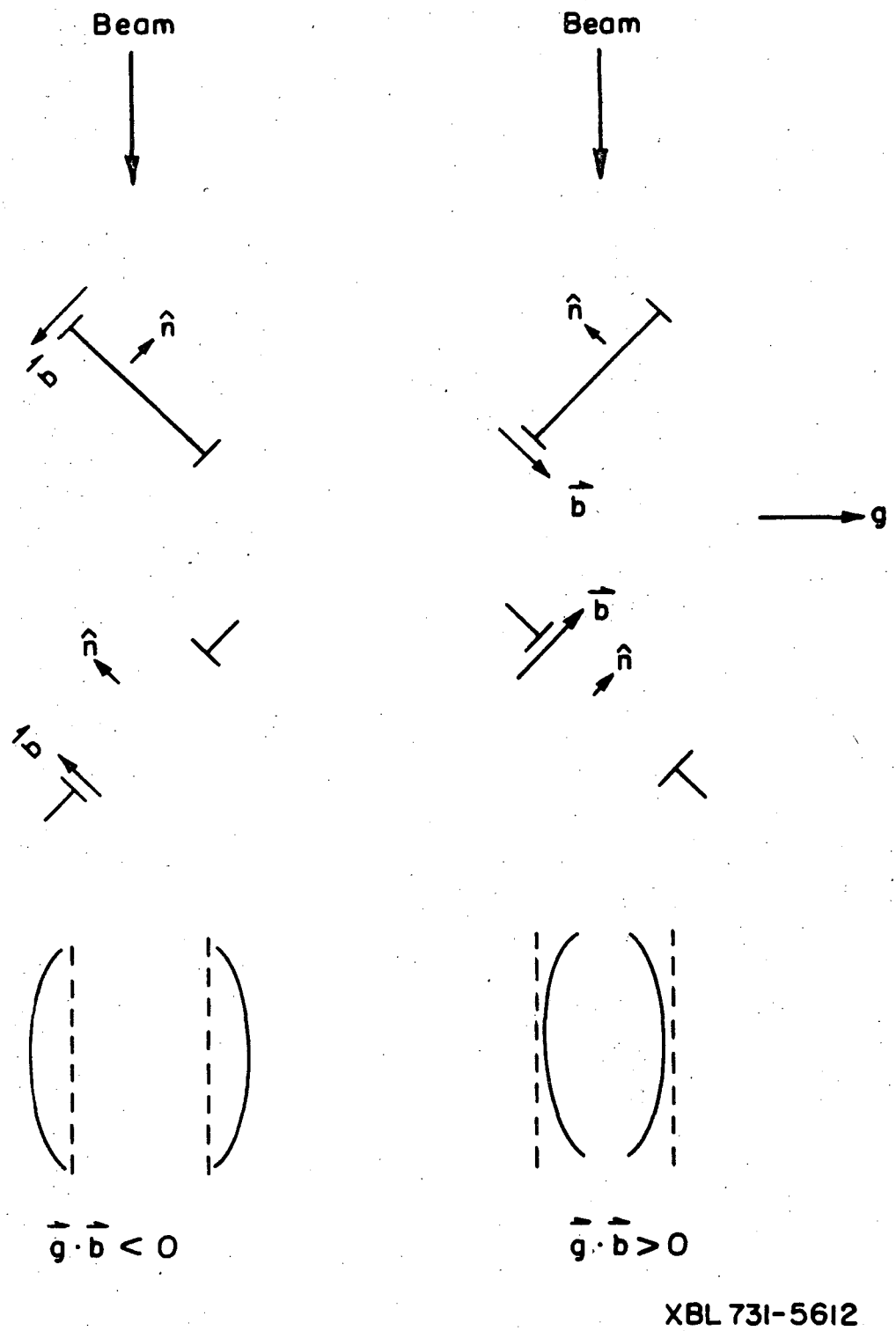
Beam
Beam
$\hat{n}$
$\vec{b}$
$\vec{g}$
$\vec{g}\cdot\vec{b} < 0$
$\vec{g}\cdot\vec{b} > 0$
XBL 731-5612

Fig. 2

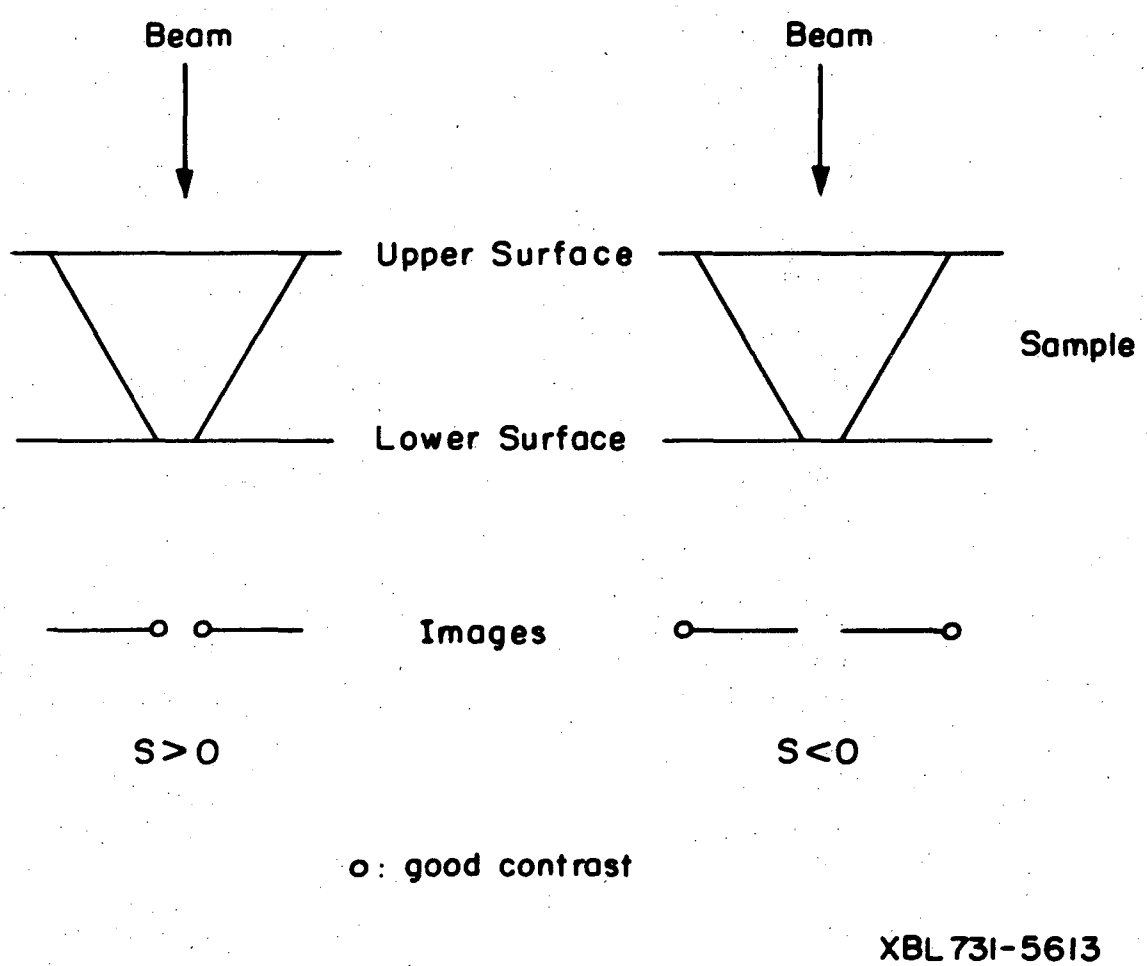
Beam
Beam
Upper Surface
Sample
Lower Surface
Images
S>0
S<0
o: good contrast
XBL 731-5613

Fig. 3

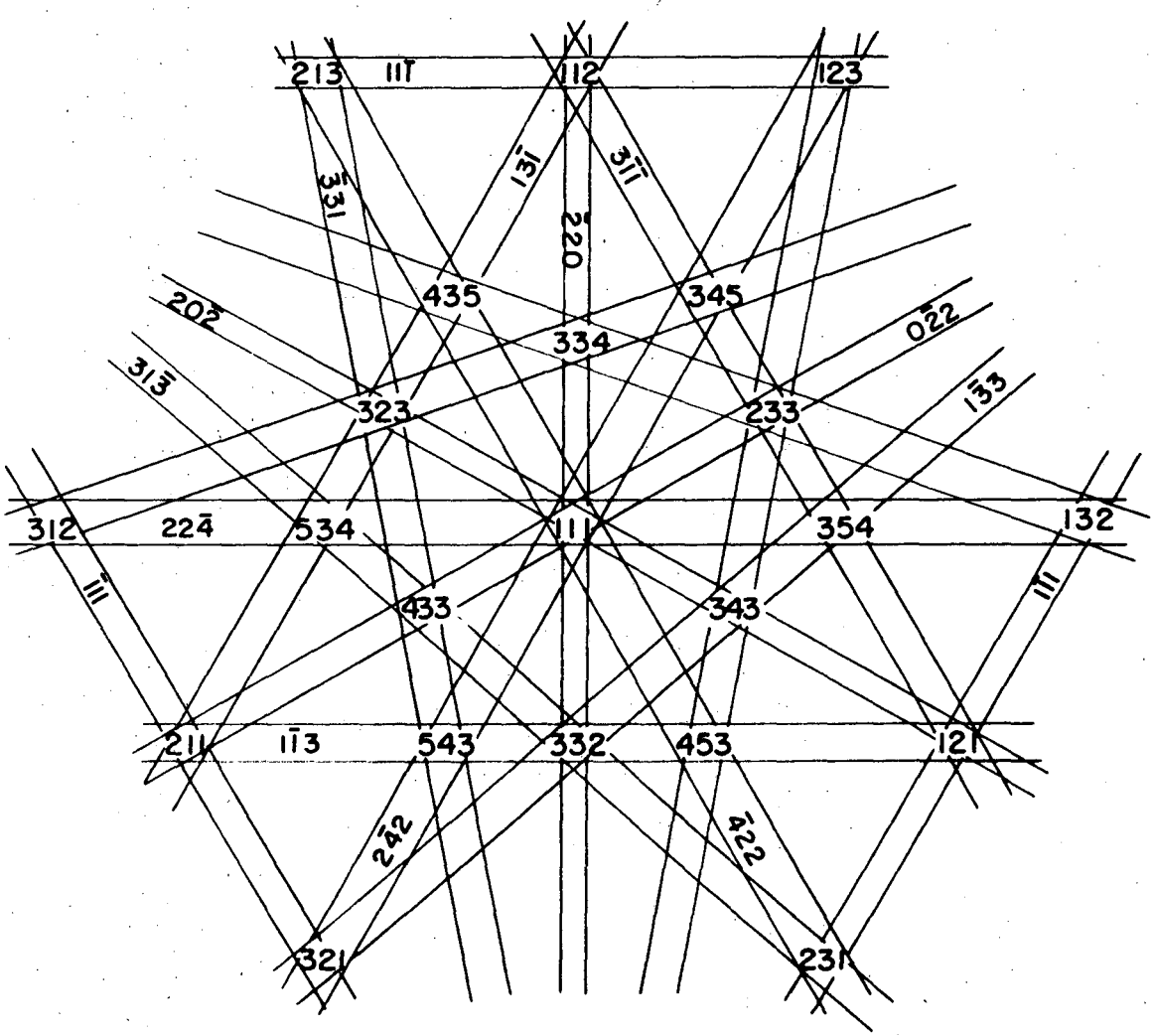

XBL 731-5614

Fig. 4

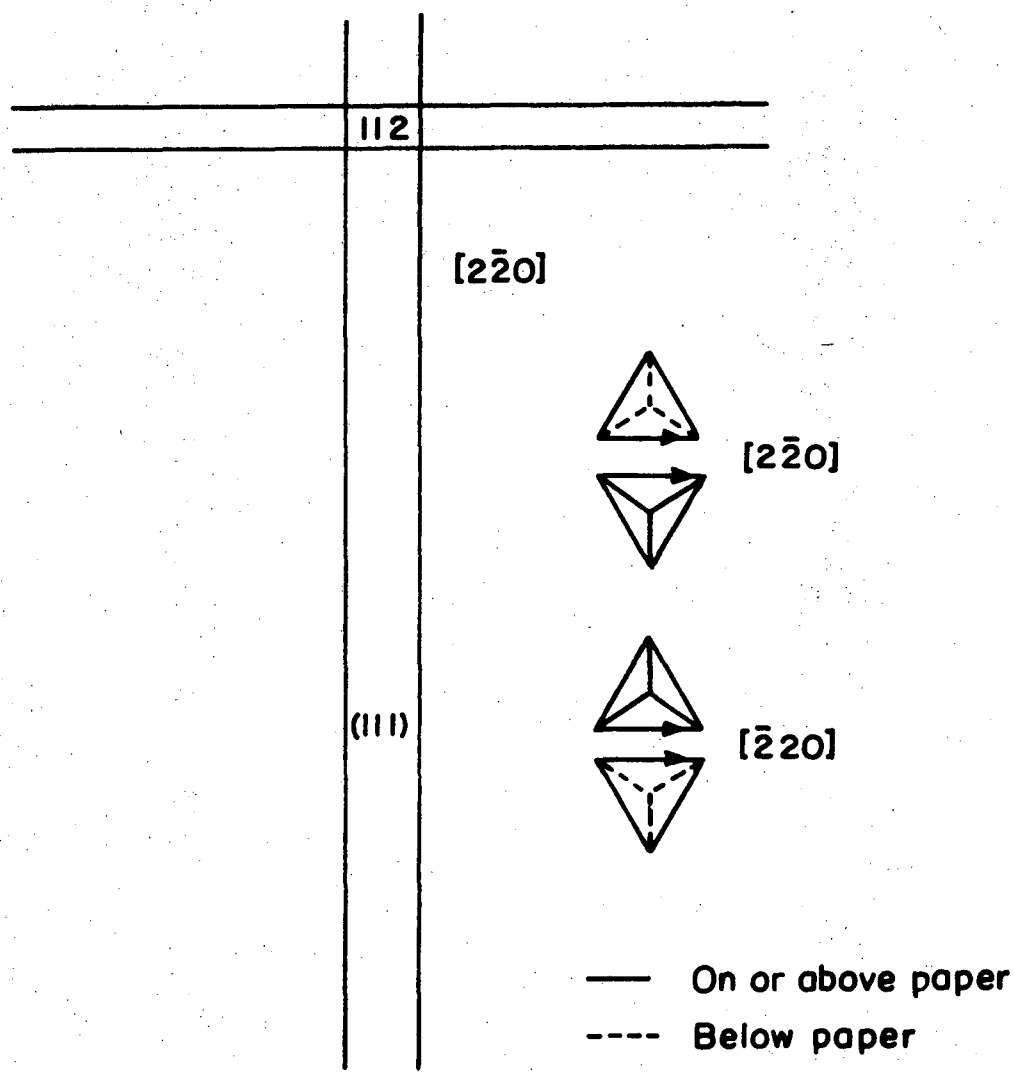

XBL731-5615

Fig. 5

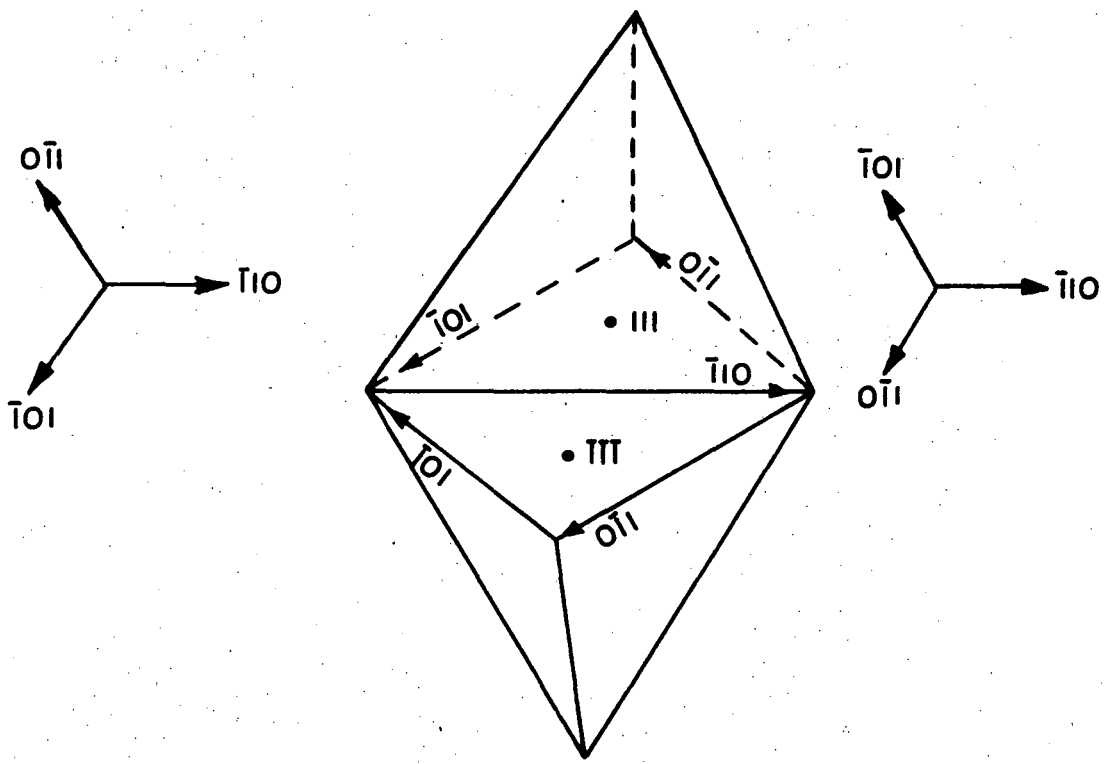

XBL731-5616

Fig. 6

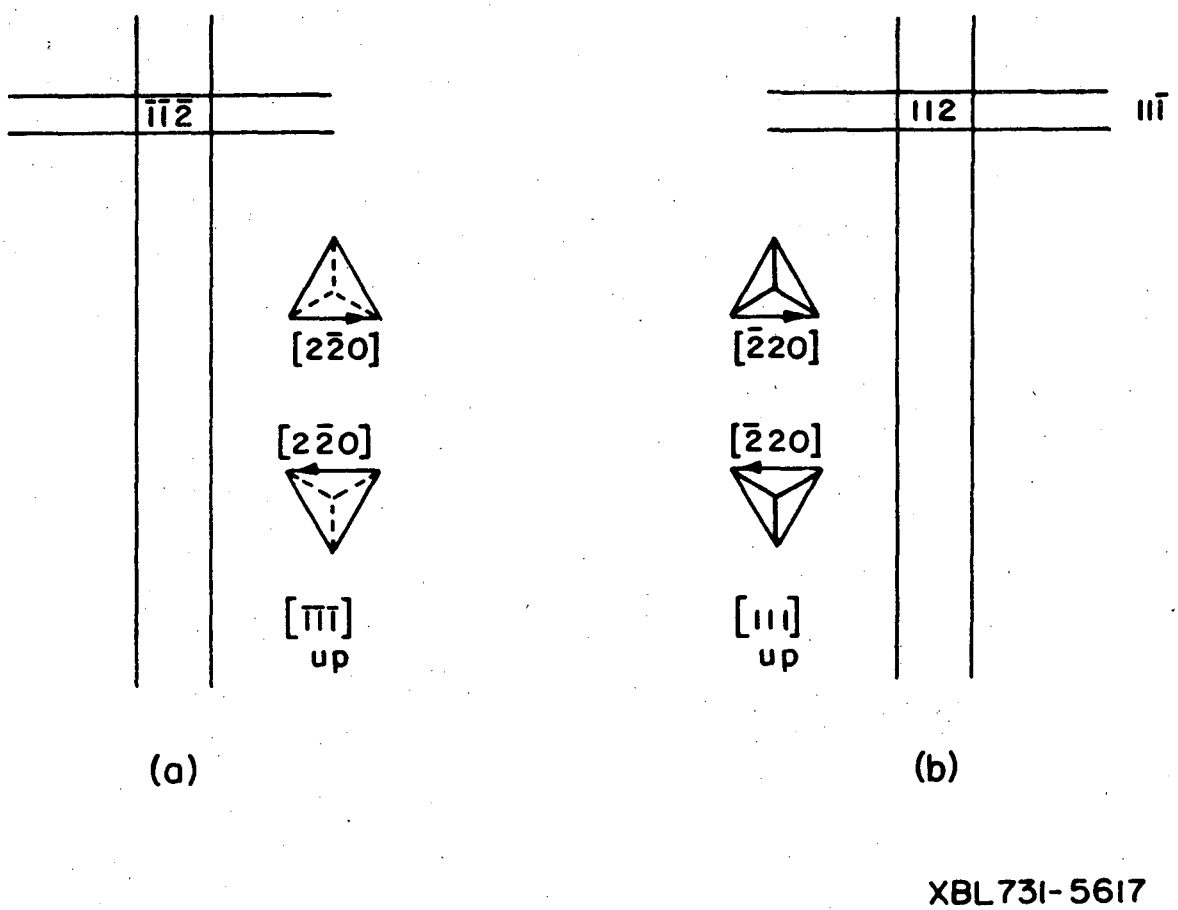

XBL731-5617

Fig. 7

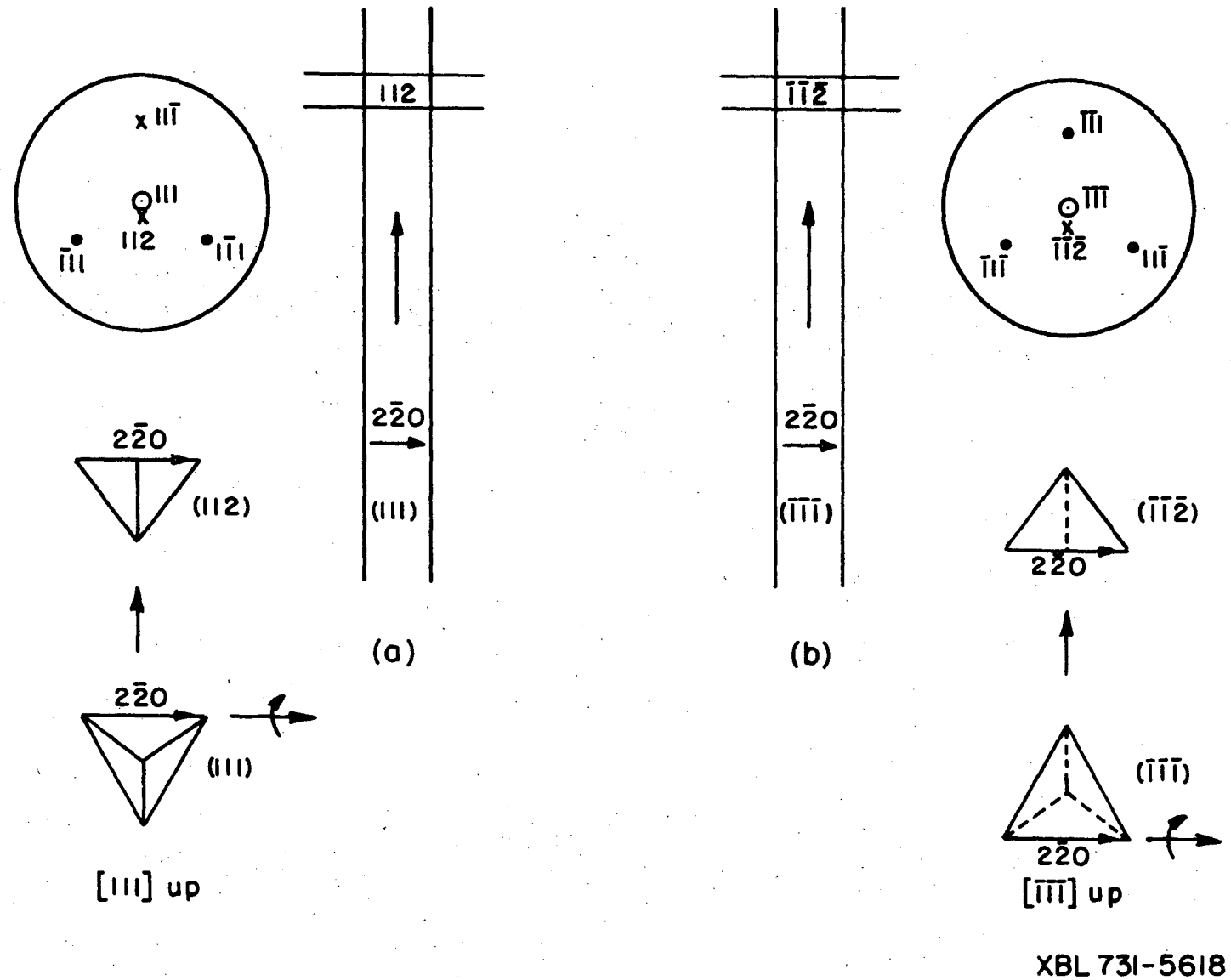

XBL 731-5618

Fig. 8

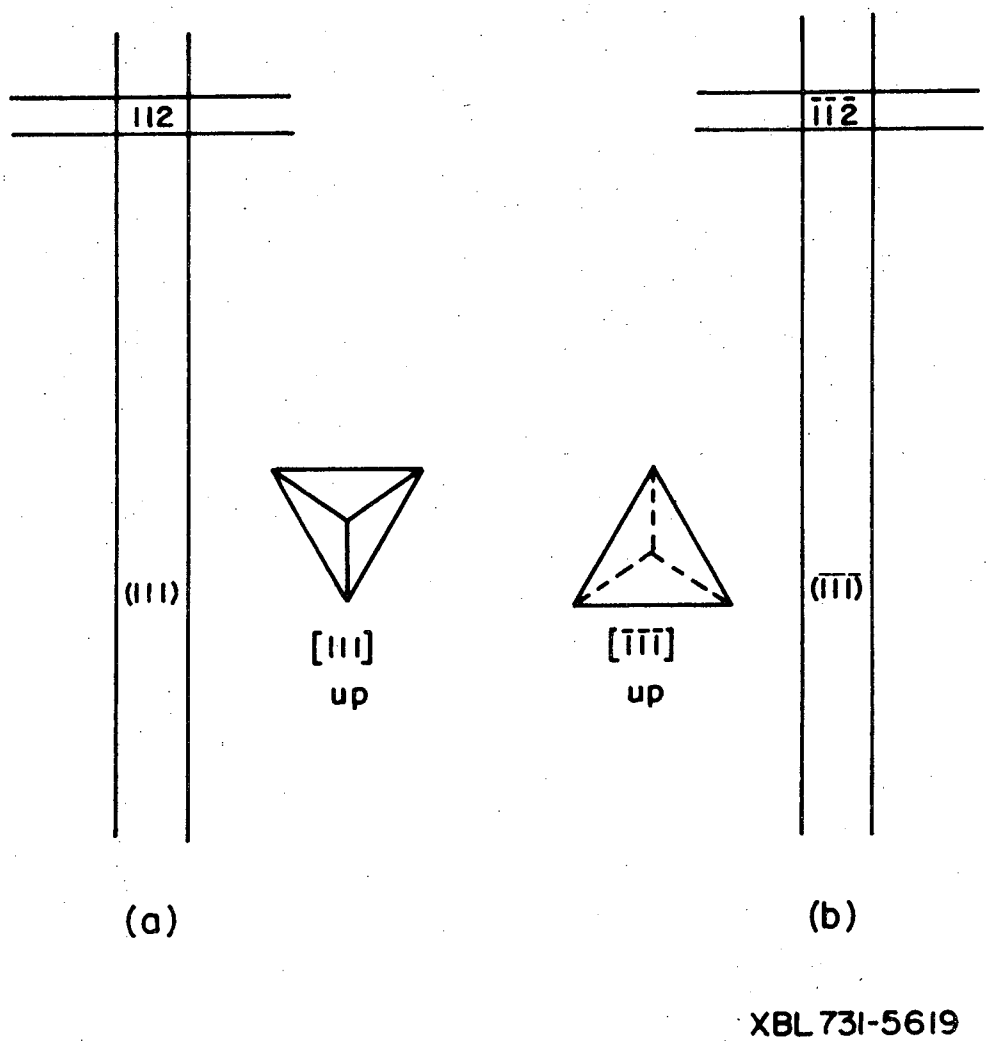

XBL 731-5619

Fig. 9

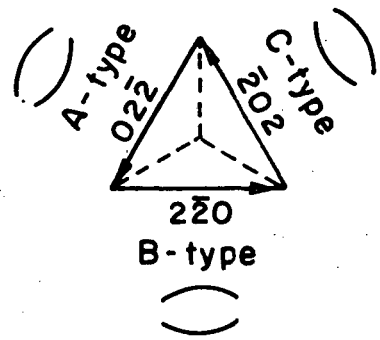

Interstitial Type

	A-type	B-type	C-type
$g = 2\bar{2}0$	outside contrast	------	inside contrast
$g = 02\bar{2}$	------	inside contrast	outside contrast
$g = \bar{2}02$	inside contrast	outside contrast	------

Vacancy Type

	A-type	B-type	C-type
$g = 2\bar{2}0$	inside contrast	------	outside contrast
$g = 02\bar{2}$	------	outside contrast	inside contrast
$g = \bar{2}02$	outside contrast	inside contrast	------

XBL731-5672

Fig. 10

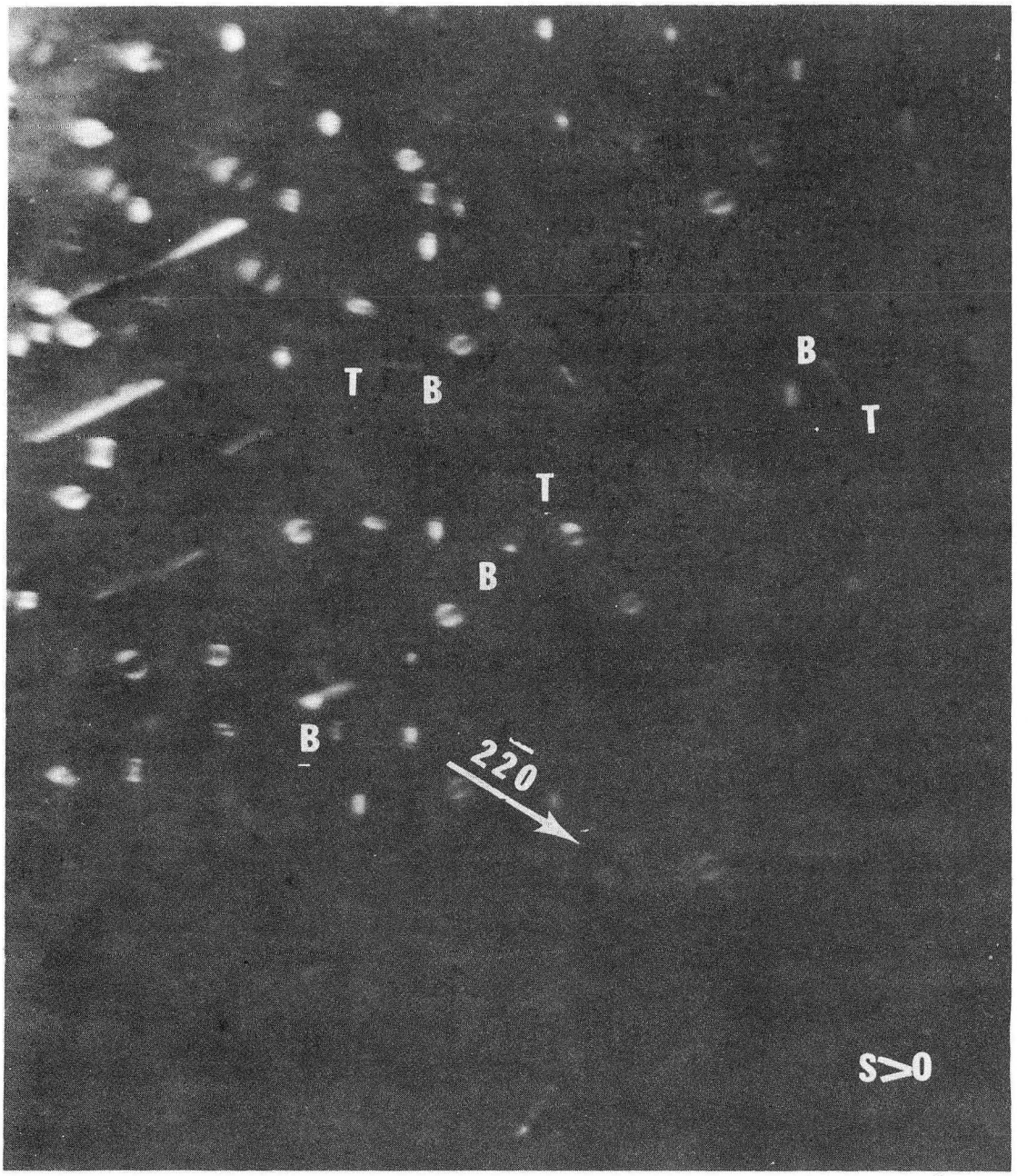

XBB 7212-6223

Fig. 11

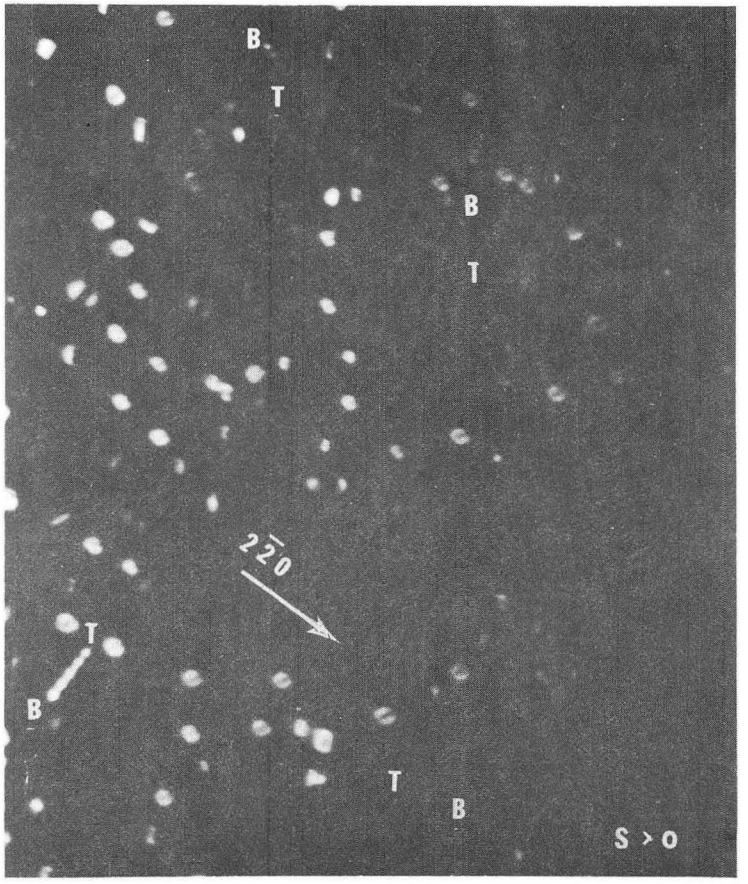

a

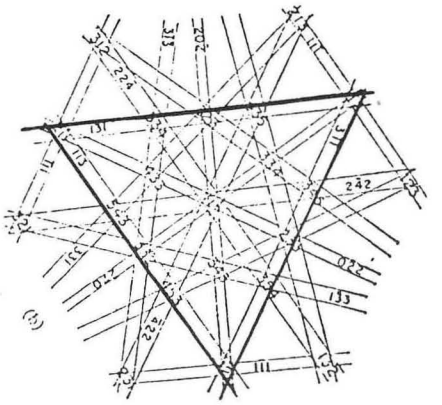

b

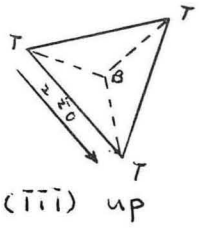

c

XBB 7212-6232

Fig. 12

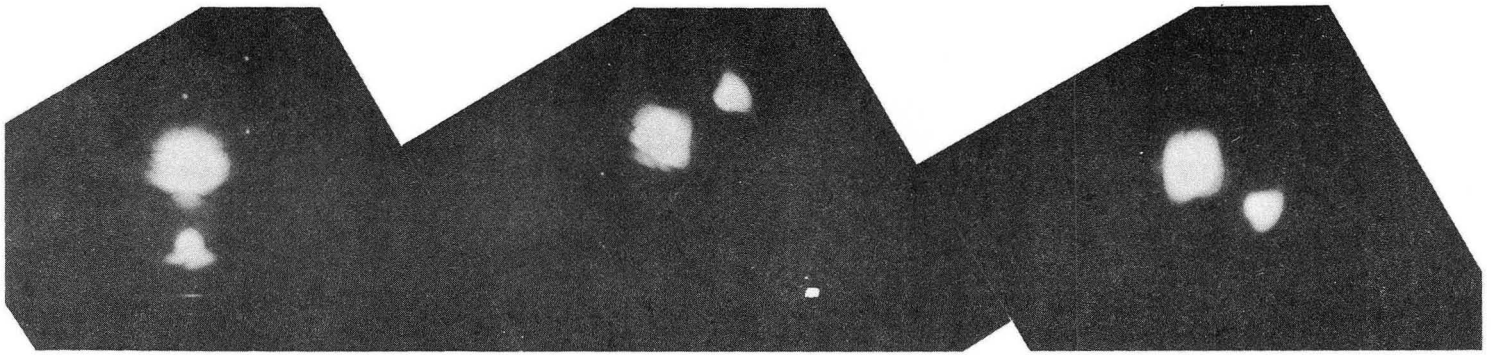

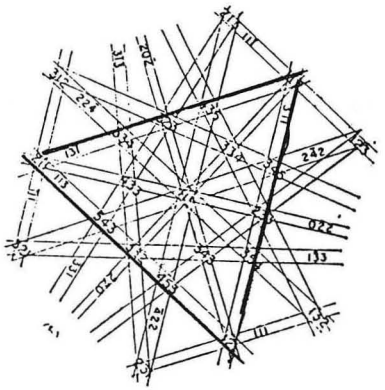

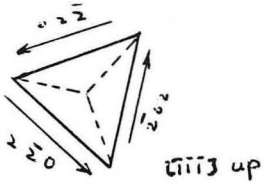

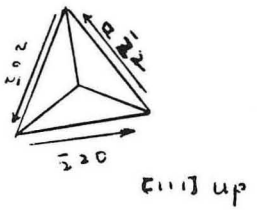

XBB 7212-6233

Fig. 13(a)

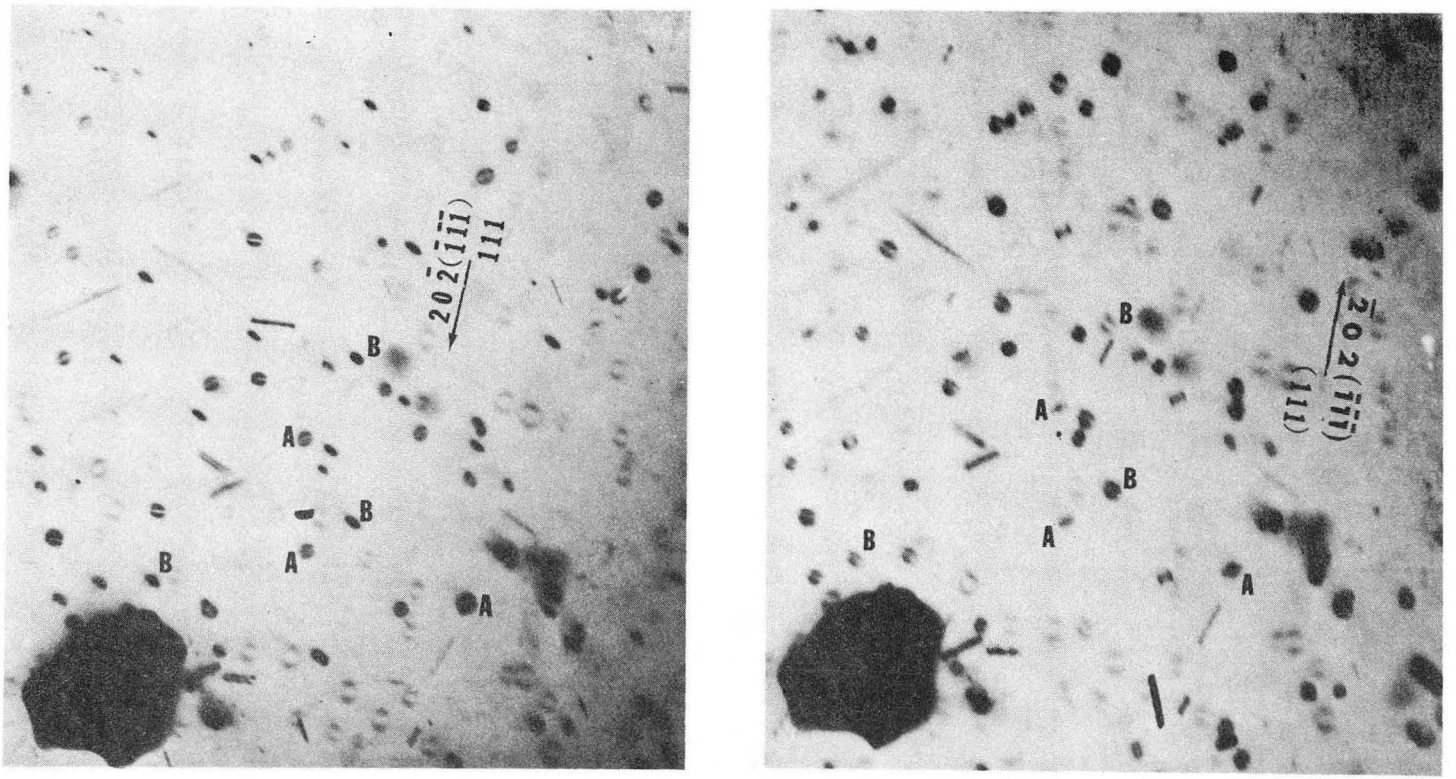

XBB 7212-6229

Fig. 13(b)

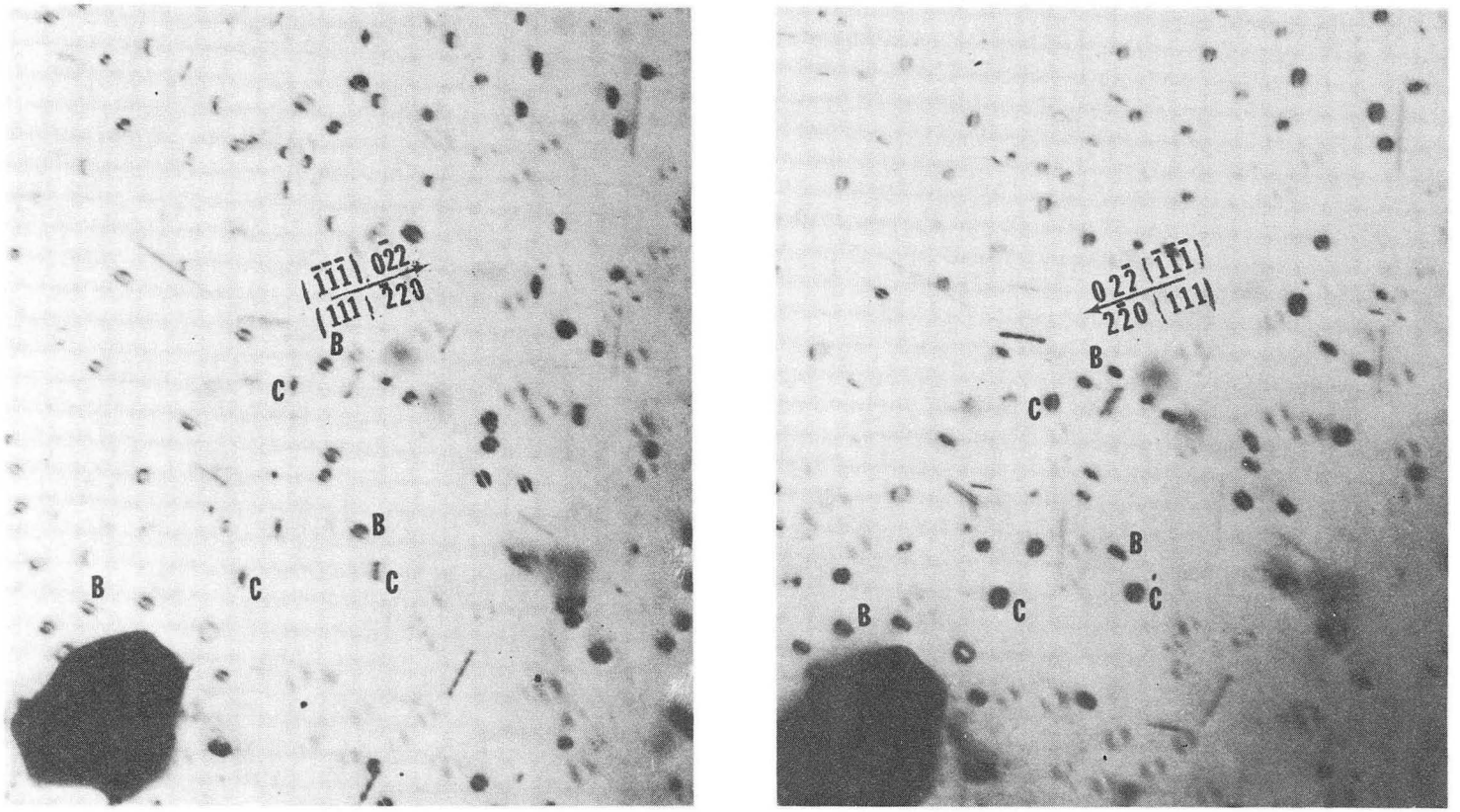

XBB 7212-6226

Fig. 13(c)

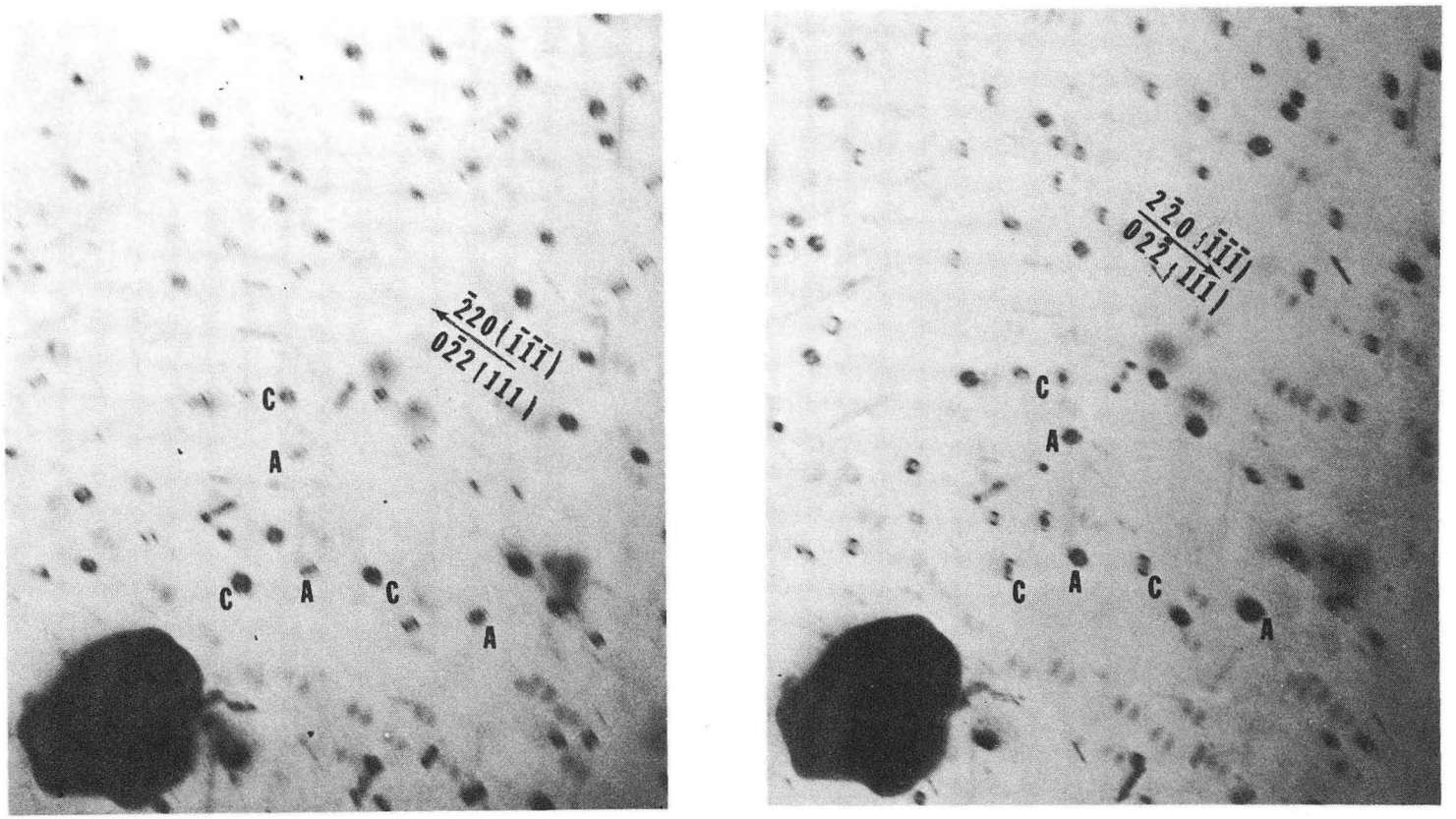

XBB 7212-6224

Fig. 13(d)

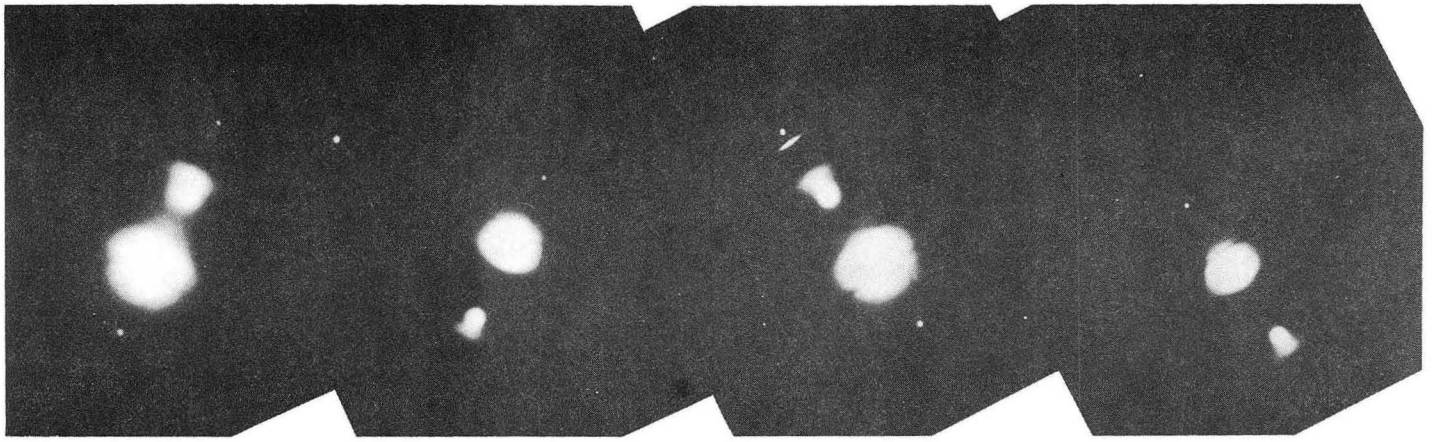

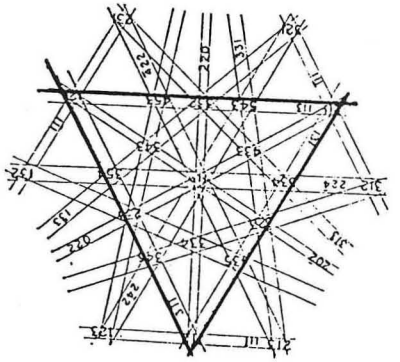

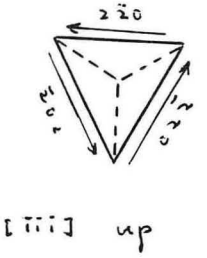

XBB 7212-6234

Fig. 14(a)

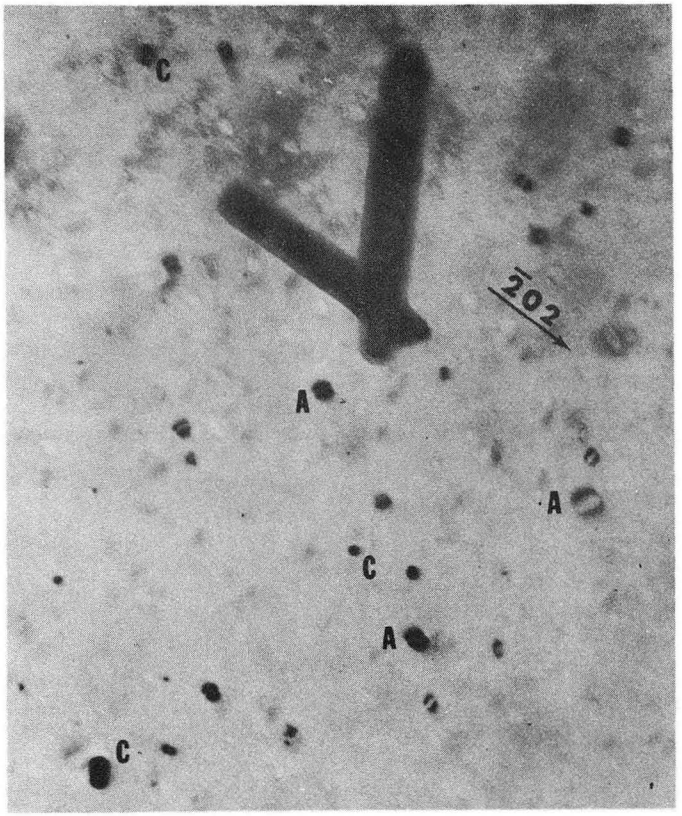

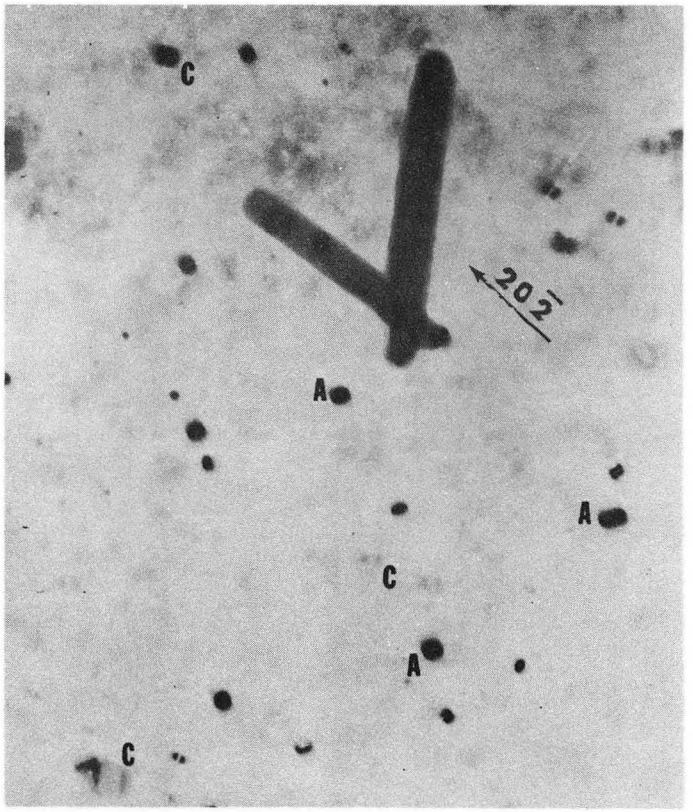

XBB 7212-6225

Fig. 14(b)

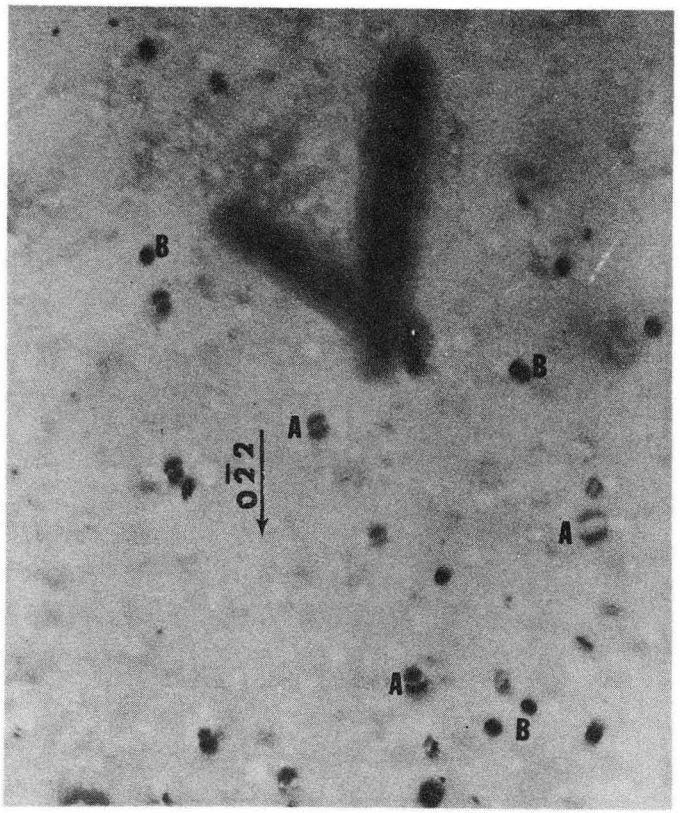

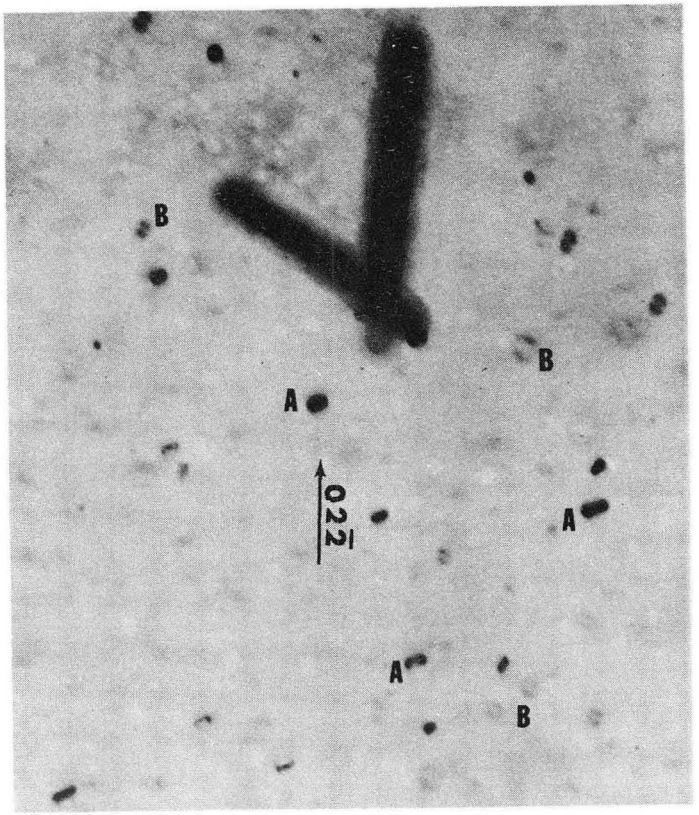

XBB 7212-6227

Fig. 14(c)

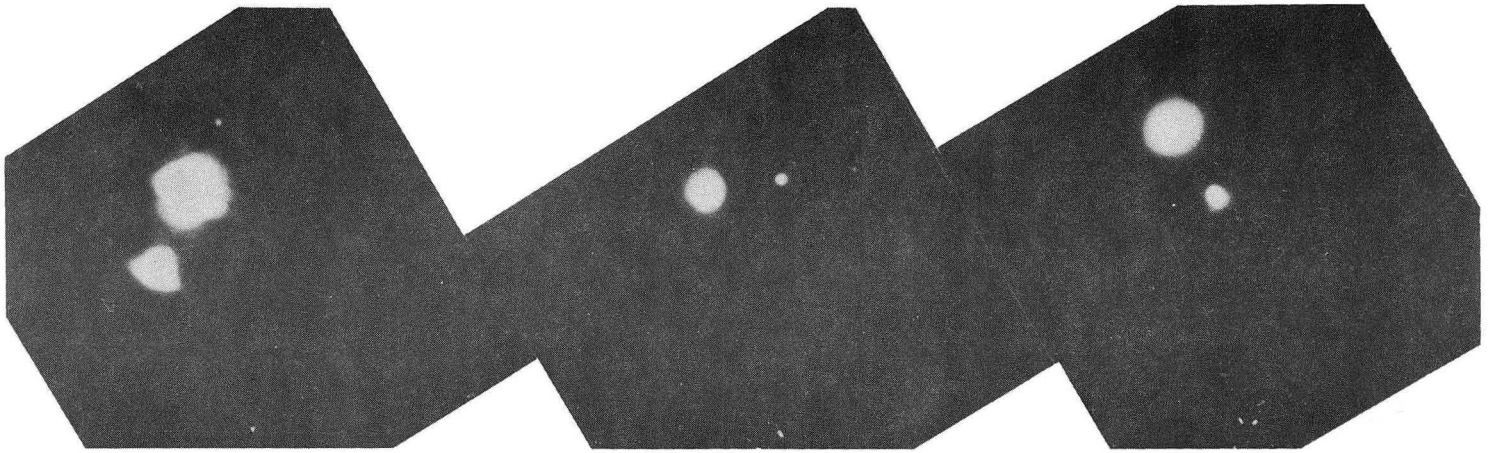

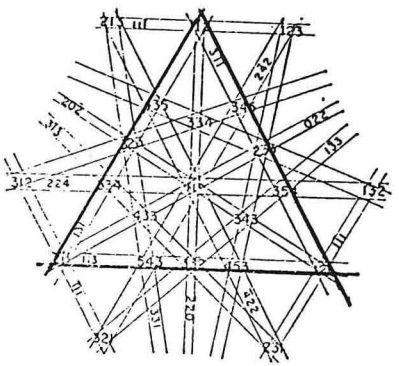

XBB 7212-6235

Fig. 15(a)

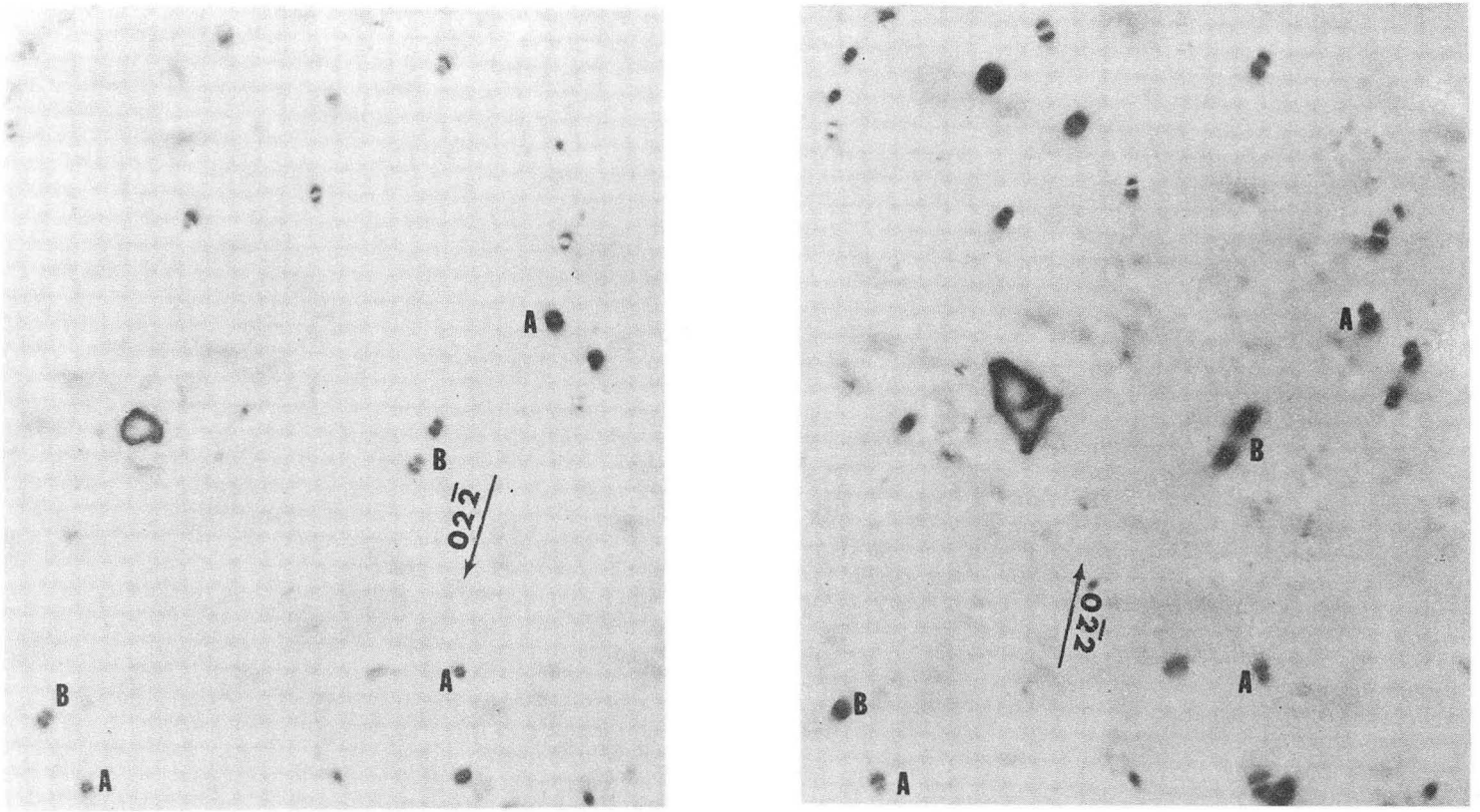

XBB 7212-6230

Fig. 15(b)

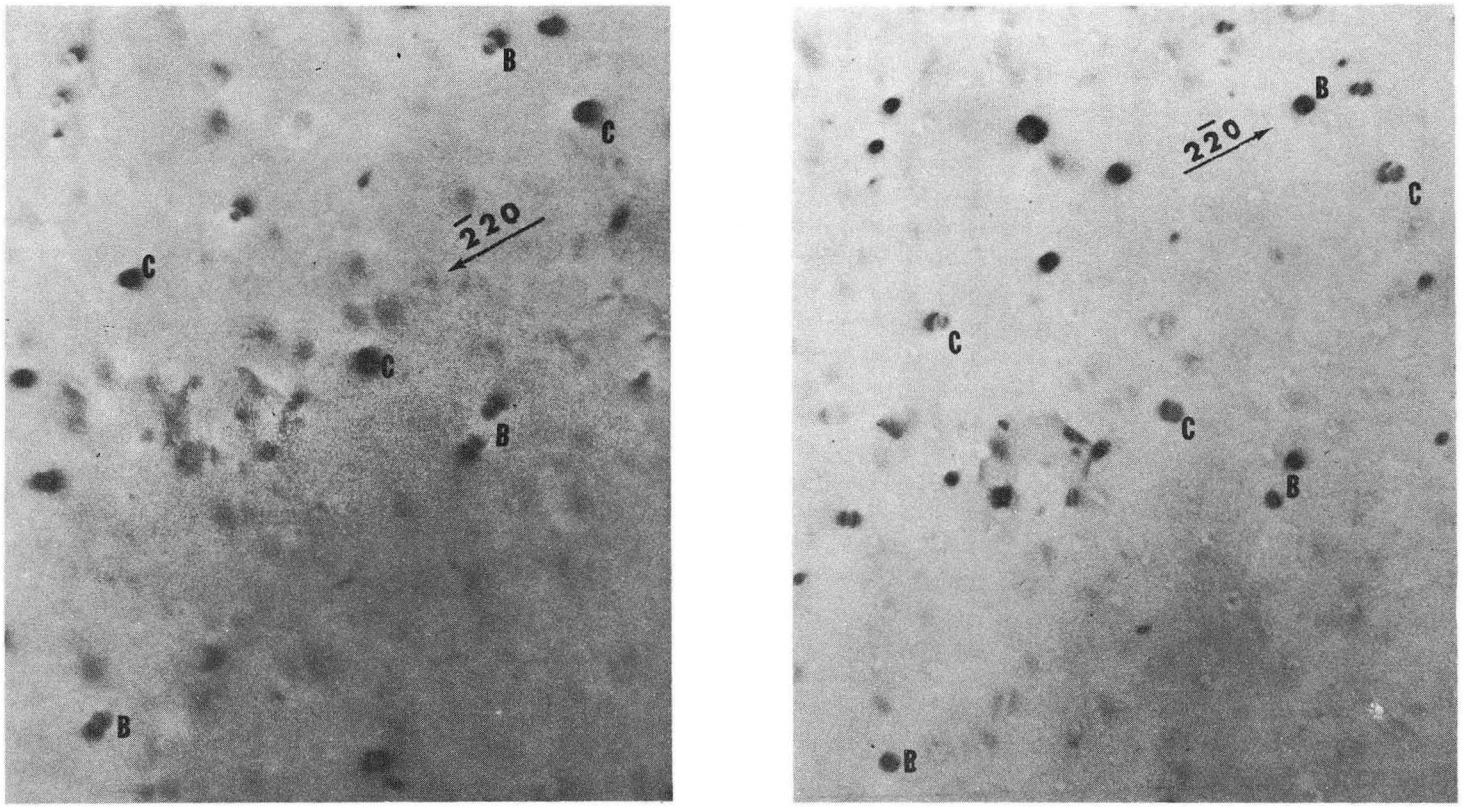

XBB 7212-6228

Fig. 15(c)

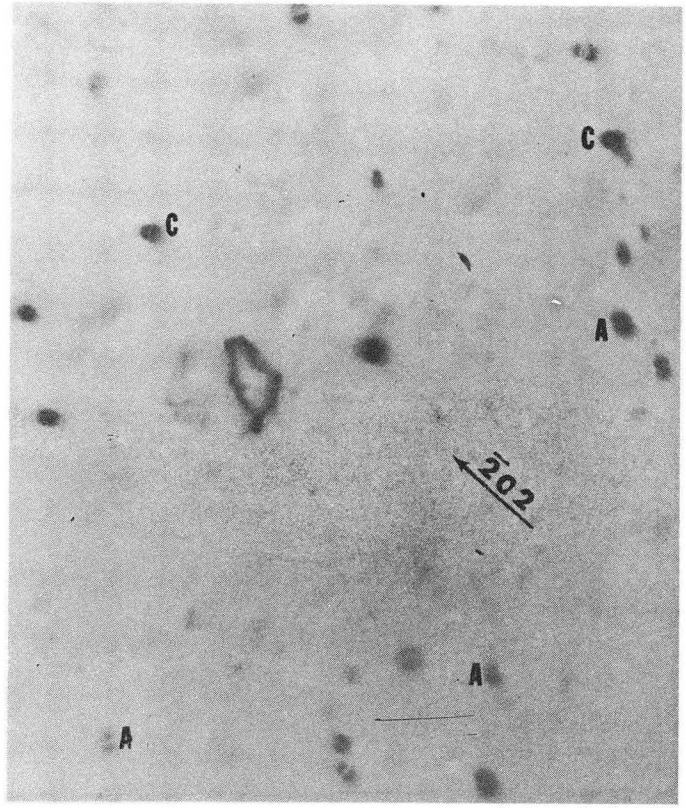

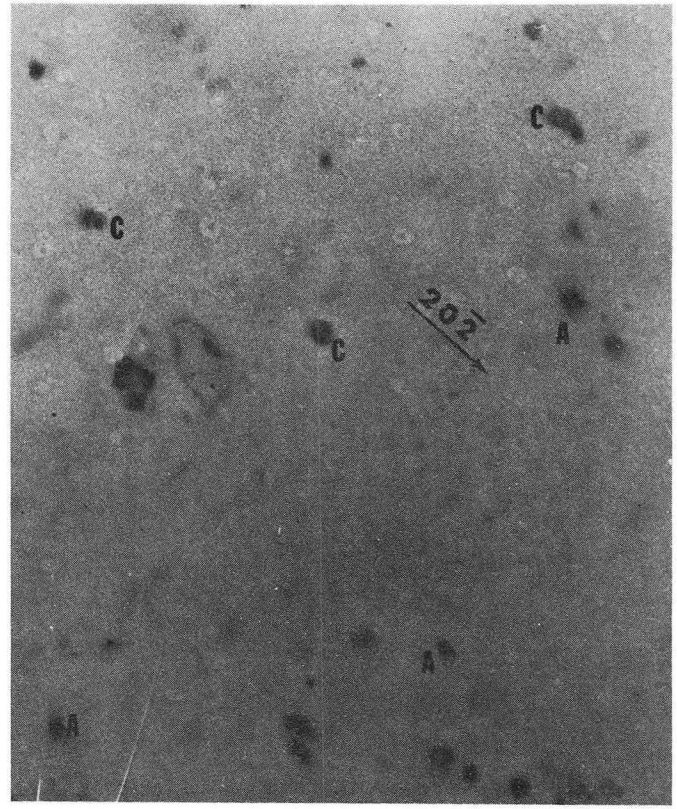

XBB 7212-6231

Fig. 15(d)

LEGAL NOTICE

This report was prepared as an account of work sponsored by the United States Government. Neither the United States nor the United States Atomic Energy Commission, nor any of their employees, nor any of their contractors, subcontractors, or their employees, makes any warranty, express or implied, or assumes any legal liability or responsibility for the accuracy, completeness or usefulness of any information, apparatus, product or process disclosed, or represents that its use would not infringe privately owned rights.

TECHNICAL INFORMATION DIVISION
LAWRENCE BERKELEY LABORATORY
UNIVERSITY OF CALIFORNIA
BERKELEY, CALIFORNIA 94720